

# A Ray Tracing Approach to Capillary-Based Backscattering Interferometry

September, 2022  
Page 1



## ABSTRACT

Capillary-based backscattering interferometry has been used as a highly sensitive refractive index sensing tool to measure molecular binding. Generally, ray tracing is used to simulate the backscattered light from the specific capillary. Previous ray tracing models do not account for polarization effects, capillary dimensions and material choices, and other parameters that could change the interference patterns captured. Researchers from the United Kingdom have developed a comprehensive ray tracing model including many parameters not previously reported. The significance of the inner diameter, outer diameter, and the refractive index of the capillary material are shown to heavily influence the interference pattern. Potential designs are explored to measure sensitive temperature changes, and therefore refractive index changes, based on capillary characteristics.

## BACKSCATTERING INTERFEROMETRY

Backscattering interferometry (BSI) is a technique of capturing light from a source (typically a laser) that has reflected, refracted, or scattered back from a solution under study. Fringe patterns from the backscattered light, can be utilized as a refractive index sensor with extremely high accuracy. Capillary-based BSI is common for measuring molecular binding through sensing refractive index changes. Typically, capillaries are hollow glass tubes with a circular geometry. **Figure 1** shows a typical capillary-based BSI setup with the different first-order rays that are possible in the capillary geometry.

Depending on the angle of incident light and the index of refraction of the capillary material and solution, certain rays of light may not ever be backscattered to the detector or

camera. This can be seen by the 'x' located in the top capillary in **Figure 1**.

Although capillary-based BSI is very successful in analyzing different refractive index scenarios, it is generally lacking in literature for clarification on experimental parameters: effects of the polarization state of the incident light and capillary dimensions on the final fringe pattern.<sup>1</sup> Some researchers have developed ray tracing models and simulations, however, these models can seem contradictory in specific situations.

Ray tracing is an optical simulation model for determining the final location and propagation of light rays through a given system. Amplitude, optical phase, and propagation direction can be determined analytically with this technique.<sup>1</sup> **Figure 1** shows the results of propagation in ray tracing.

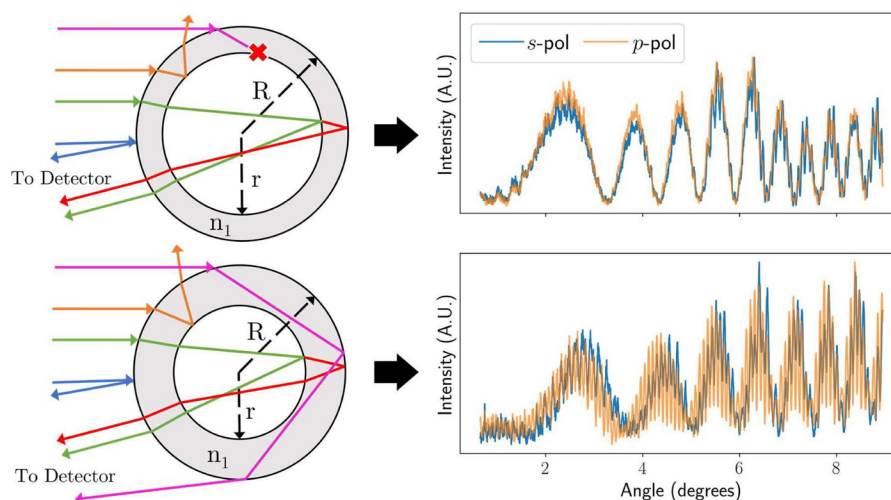


**Figure 1. Capillary-based backscattering interferometry setup with different first-order rays that are possible in the capillary geometry and the angle of incident vs. intensity of the backscattering signal with different polarizations.<sup>1</sup>**

## PROBLEMS AND GOALS

There are two main parameters in capillary-based backscattering interferometry (BSI): the angle of the incident light and the geometry of the capillary. Both the angle of incident light and the geometry affect the light rays detected by the camera and the intensity of the backscattered light. The most common geometry for BSI is a circular hollow glass tube. However, some experiments have carried out BSI using semicircular microfluidic channels. While this geometry of capillary may be easier to analyze theoretically due to its similarities to Fabry-Perot etalons and Michelson interferometers, the manufacturing costs can be significantly higher and the increase in sensitivity and stability are only minimal.<sup>1</sup>

**Figure 2** shows the cross section of a basic, circular, hollow tube geometry. Overlaid on this diagram are the different first-order rays possible given this particular geometry of the capillary.

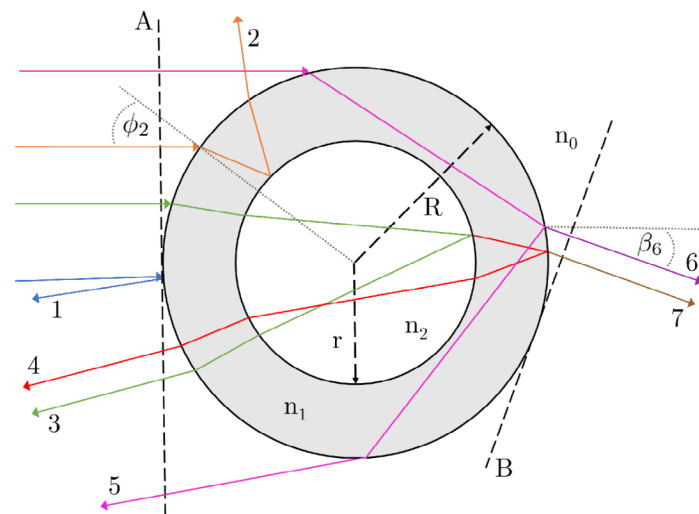


**Figure 2.** A diagram showing the different first-order rays that are possible in the capillary geometry of BSI. The incident angle of a given ray  $\phi_i$  is simply the angle to the surface normal. In the Xu/You et al.'s methodology, the angle of incidence is related to the viewing angle  $\beta_i$  of each ray, where  $\beta_i$  is defined to be the angle to the horizontal in this geometry. The example of  $\beta_6$  is shown here. The diagram is adapted from Ref. 2.<sup>2</sup> The rays are demonstrative and not drawn with geometric accuracy.<sup>1</sup>

Both **Figure 1** and **Figure 2** show that the angle of incidence determines what rays of light are backscattered as well as the intensity of the captured light. In two previous ray tracing models<sup>3,4</sup>, there is a discrepancy regarding which rays to include. Tarigan et al.<sup>4</sup> uses a four beam model with rays 1, 2, 3, and 4 in **Figure 2**, while Xu et al.<sup>3</sup> and You et al.<sup>2</sup> use a model with all seven beams in **Figure 2**. This

discrepancy of which rays are considered relevant between the two models creates a problem of choosing the more accurate and more sensitive model for BSI. Because rays 6 and 7 do not contribute to the signal seen at the detector, only the omission of ray 5 will need to be justified. Models with more than 5 rays exist, but they are confined to commercial software.<sup>1</sup>

Critical parameters that influence the resulting fringe pattern of the backscattering are:

$r$  = Inner radius of the hollow glass tube capillary

$R$  = Outer radius of the hollow glass tube capillary

$n_0$  = Refractive index of air/outside the capillary

$n_1$  = Refractive index of the capillary

$n_2$  = Refractive index of the solution inside the capillary

$\phi_i$  = Incident angle of a given ray (i) to the surface normal

$\beta_i$  = Output or viewing angle of a given ray (i) to the surface normal

A new and unified model, backed by experimental data, needs to be created for non-commercial use that states the effects of multiple capillary parameters. Previous models do not account for all seven first-order rays, the polarization state of the incident light, and the dimensions and material of the capillary.

## METHOD

Researchers from the University of Bristol, UK have developed a new ray tracing model for analyzing fringe patterns of a hollow glass tube capillary. Two previous ray tracing models are combined to create one composite model for more general use. Through this simulation model and experiment data, researchers can better understand and improve the sensitivity of backscattering interferometry. The effects of the polarization of the incident light and the characteristics of the capillary are thoroughly examined.

The experimental apparatus can be seen in **Figure 3**. A 7 mW laser passed through a filter, fiber, and a linear polarizer to obtain a single spatial mode with a variable linear polarization state. The light is incident onto the circular glass capillary with outer radius  $R$  and inner radius  $r$  with refractive index  $n_1$ . The capillary, containing a liquid of refractive index  $n_2$ , is held on a custom aluminum stage with constant temperature control from a Peltier thermoelectric module controlled by Wavelength Electronics' WTC3243HB temperature controller. The light that is backscattered or reflected and refracted from the capillary in a direction anti-parallel to the incident light creates an interference pattern collected by the camera.<sup>1</sup> The interference pattern is recorded and can change/move laterally due to fluctuations

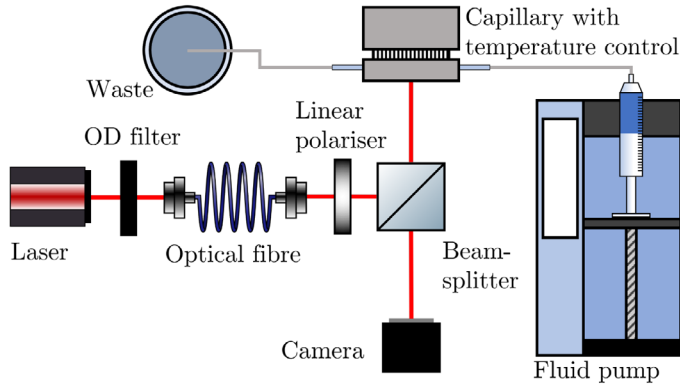


**Figure 3. A schematic diagram of the backscattering interferometry apparatus used in this work.<sup>1</sup>**

in the refractive index of the liquid inside the capillary. A Fourier transform of the intensity pattern is used to monitor the fringe translation by using the phase change of the desired frequency peak of the Fourier transform.

For the desired unified ray tracing model, the Xu<sup>3</sup>/You<sup>2</sup> and Tarigan<sup>4</sup> methods are combined and adapted. The largest discrepancy between the two models is the omission of ray 5. Using Snell's law and other geometrical arguments, the viewing angle  $\beta_5$  can be shown in terms of  $\phi_5$  and known constants:

$$\beta_5 = 2\phi_5 - 4 \arcsin\left(\frac{\sin\phi_5}{n_1}\right) + \pi$$

which is valid where  $\arcsin(n_1 r/R) \leq \phi_5 \leq \pi/2$ . At  $\rho = n_1 r/R > 1$ , ray 5 will cease to exist due to the inner diameter of the capillary blocking the ray.<sup>1</sup> For this particular capillary made of fused silica, a typical refractive index with be  $n_1 \approx 1.457$  at the incident wavelength of 632.8 nm. This means that  $r/R < 0.68$  for ray 5 to be valid and contribute to the interference patterns. At  $r/R \geq 0.68$ , ray 5 is no longer defined or included in the interference with any backscattered rays. The Tarigan<sup>4</sup> model uses a capillary above this limit and so, correctly, does not consider ray 5 in the experiment. In many cases, the refractive index of the capillary is unknown, making the  $r/R = 0.68$  just an estimate.<sup>1</sup>

Other factors, taken into account in one or both models, are also shown to be either case specific or incorrect. For example, the Tarigan<sup>4</sup> model uses the small angle approximation which is justified when only considering rays 1, 2, 3, and 4, but if  $r/R < 0.68$ , the small angle approximation cannot be considered for ray 5. The other model assumes that the refractive index of the solution inside the capillary is higher than the capillary itself,  $n_2 > n_1$ . This is not typically the case in the average BSI experiment. For correction, the angular bounds of rays 3, 4, and 7 can be adjusted.<sup>1</sup>

Once the incident angle  $\phi_i$  and viewing angle  $\beta_i$  are converted, the overlapping beams interfere pairwise to create the fringe patterns. Because this model does not only consider small angles and the correlating approximations, the reflection and transmission are angle- and polarization-dependent. Researchers use the amplitude versions of the reflection and transmission coefficients to model phase changes upon each reflection and transmission, rather than the typical intensity version which does not account for any phase changes.

## RESULTS

With the new unified model, both methods were replaced by the full polarization-variable formulations in amplitude rather than intensity.<sup>1</sup> A fast Fourier transform was implemented to aid in the analysis. The most obvious result is the difference in fringe patterns seen for  $\rho = n_1 r/R < 1$  and  $\rho = n_1 r/R > 1$  capillaries. These parameters refer to when ray 5 does and does not contribute to the interference patterns seen, respectively. In some figures, when  $\rho > 1$ , it will be referred to as high  $\rho$ . When  $\rho < 1$ , it will be referred to as low  $\rho$ .

**Figure 4** shows the simulated interference patterns for both high and low  $\rho$  capillaries. Both s- and p-polarized incident light are present across a range of viewing angles.

**Figure 5** shows the experimentally obtained interference patterns with the same parameters listed in **Figure 4**. These patterns are collected using the apparatus in **Figure 3**.

When comparing **Figure 4A** and **Figure 5A** (high  $\rho$ ), the fringes formed at the camera resemble a two-beam interference pattern with a very low frequency envelope component.<sup>1</sup> The pattern is largely dominated by ray 1 and ray 4. Other rays cause some modulation within the pattern. When comparing the interference patterns with the correlating s- and p-polarization, there is little difference. Both in simulation and experimentally, the interference patterns are essentially polarization-independent. This is something that was not clear and perhaps unknown in the other ray tracing models.

When viewing **Figure 4B** and **Figure 5B** (low  $\rho$ ), the fringe pattern looks significantly different. Although all the parameters are kept the same, except the reduced  $\rho$  value, there is a much higher frequency fringe pattern. This can be explained from the large variation in path length of ray 5 as the incident angle is varied. Once again, the frequency envelope is maintained regardless of polarization state. However, the relative intensity is slightly lower for the s-polarization. Although the polarizations results are slightly different, in general experiments the polarization state will have a negligible impact on the fringes observed.<sup>1</sup>

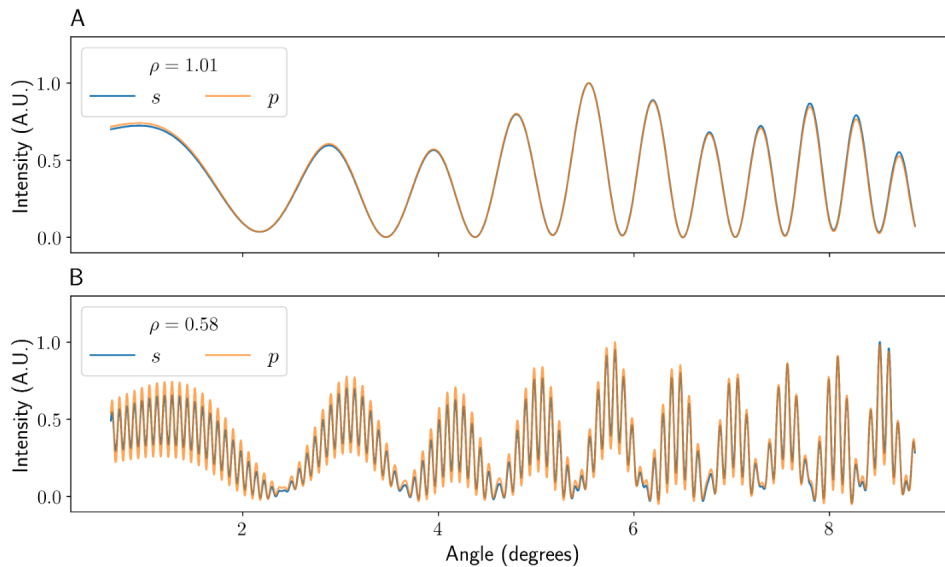


**Figure 4. A graph showing the simulated intensity patterns seen for a capillary higher (A) and lower (B) than the  $\rho = 1$  limit for both s- and p-polarized incident light. The data were taken 9 cm horizontally and 0.75 cm vertically from the capillary, with a simulated camera width of 1.3 cm. The angle is given in degrees from  $\beta = \pi$ . The data have been normalized between 0 and 1 to aid comparison.<sup>1</sup>**

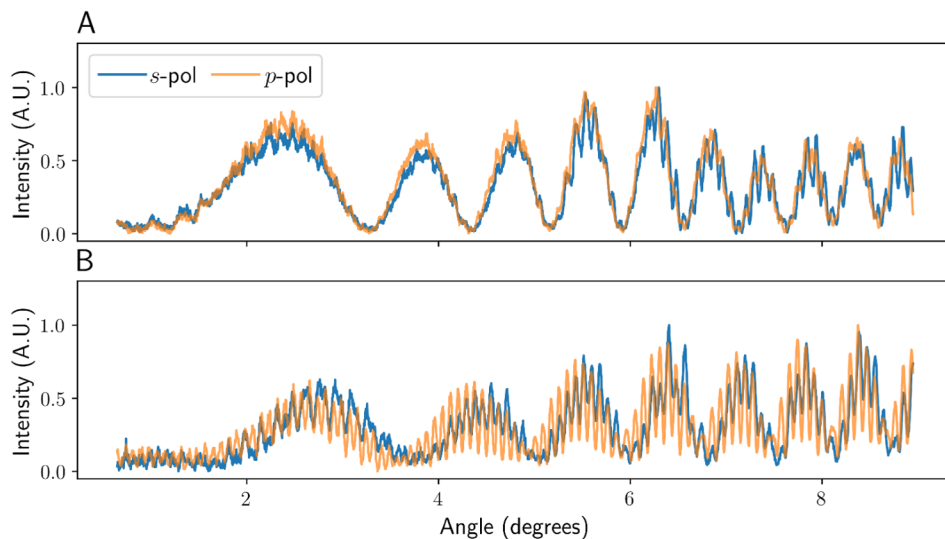


**Figure 5. A graph showing the experimental intensity patterns seen for a capillary both higher (A) and lower (B) than the  $\rho = 1$  limit. The data were taken at  $\sim 9$  cm horizontally and  $\sim 0.75$  cm vertically from the capillary, with a camera width of 1.3 cm. The data were longitudinally averaged to reduce high-frequency noise and produce a more representative fringe pattern. The data have been normalized between 0 and 1 to aid comparison.<sup>1</sup>**

In the high  $\rho$  cases, the fringe pattern is dominated by the interference between beams 1, 4, and 5. Once again, the modulation is caused by the other components. The experimental data captured here matches simulation data quite well. Any slight shifts in oscillations are most likely due to minor misalignments or manufacturing tolerances in the capillaries used.

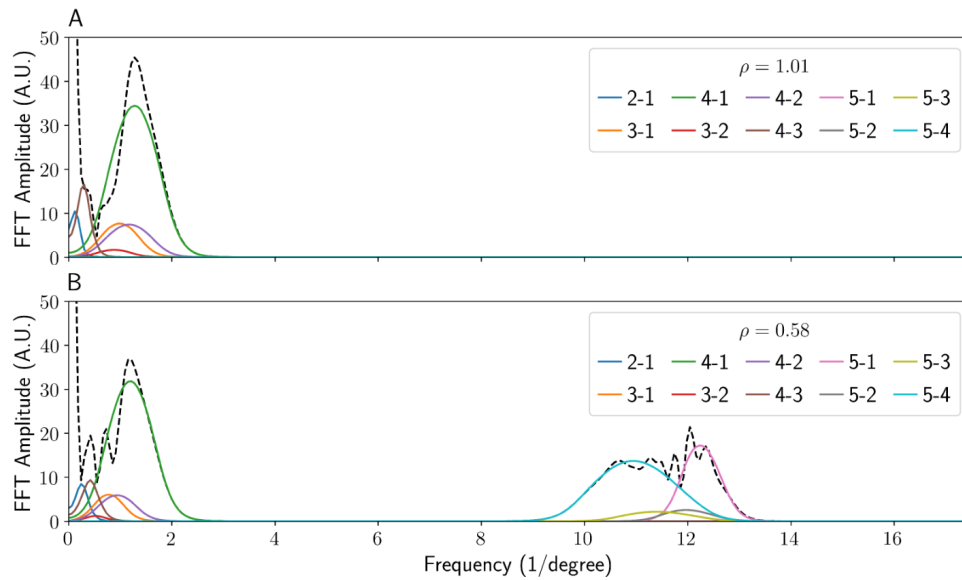


**Figure 6.** A graph comparing the Fourier transforms of both the high (A) and low (B)  $\rho$  values. The data were taken at 10 cm horizontally and 1 cm vertically from the capillary with a fixed camera width of 1.3 cm. The black dashed lines show the overall Fourier transforms of the patterns shown in Figure 3, with each pairwise interference term transformed and shown separately. For example, the interference between rays 1 and 2 is shown in blue and labeled 2-1. The data were windowed and zero-padded to reduce ringing and other artifacts after transformation.<sup>1</sup>

The last step in processing the collected data was to apply the fast Fourier transforms to the interference fringe patterns. **Figure 6** compares the Fourier transforms of both the high and low  $\rho$  values. Both the Fourier transforms of the simulated and experimental data match well.

In **Figure 6A&B**, it becomes obvious that the fringe pattern is dominated by only a few rays. In the high  $\rho$  plot, the "4-1" pair interference dominates the low frequency. Because many of the pairs of beams have a very similar frequency, the phase of this single peak determines how the refractive index of the liquid  $n_2$  changes during the course of the experiment. This is one way to monitor the solution refractive index with extreme sensitivity.

The "4-1" pair is also the dominating factor in the low  $\rho$  plot, again in the low frequency domain, but the higher frequency is dominated by the "5-4" and "5-1" pair interference. Because ray 5 has such a distinctly higher frequency and does not pass through the solution sample, it could be used to monitor environmental effects on the experiment.<sup>1</sup> Monitoring the phase changes of the "5-1" pair could lead to determining the refractive index changes of the capillary itself, which is typically dominated by temperature fluctuations. It is common for noise and drift in BSI measurements to contribute to temperature instabilities. Once a shift in the "5-1" pair is correlated to a temperature shift, the changes could be transmitted to the Peltier device to better maintain stable temperature through

the temperature controller. This, essentially, comes down to the material of the capillary.

While the system with low  $\rho$  shows helpful application in capillary refractive index changes and temperature fluctuations, a system with high  $\rho$  will generally be preferred. It is more robust and has a greater sensitivity due to longer path length through the solution inside the capillary. Either system, however, can provide useful information about the investigated solution inside the capillary.

With the newly developed ray tracing models, researchers realized and explored the effects of a variety of parameters on the interference pattern in capillary-based BSI. Researchers proved the importance of choosing the correct  $\rho = n_1 r/R$  value, whether high or low. The incorporation of ray 5 into the analysis could allow for a concurrent and highly sensitive temperature measurement of the capillary.<sup>1</sup> Regardless of the value chosen, capillary-based backscattering interferometry, with the improved ray tracing model, is shown to be valuable for a variety of applications regarding the changes in refractive index inside a capillary.



## WAVELENGTH'S ROLE

Due to temperature dependence of the refractive index of the solution inside the capillary and the capillary itself, the aluminum stage that holds the capillary needs to be maintained at a stable temperature. Wavelength Electronics' WTC3243HB temperature controller can achieve 0.0009°C temperature stability when coupled with a Peltier thermoelectric module. This controller, an adaption of the standard WTC3243 controller, operates from 3.6 V, Lithium-Ion batteries. The WTC3243HB ensured stable refractive index of the solution inside the capillary, correlating to more stable backscattering light collection from the camera and repeatable experimental data.

The WTC3243HB temperature controller can drive up to  $\pm 2.2$  A of thermoelectric or resistive heater current. Not only does the WTC3243HB have high linear stability, it has heating and cooling current limits and can support thermistors, RTDs, and IC sensors. The small size of 1.3" x 1.28" x 0.313" enables the WTC3243HB to be utilized in almost any setup and design.

The robust and reliable WTC3243HB is designed into handheld electro-optical systems, atmospheric lidar instruments, airborne instrumentation, Raman spectrometers, and medical diagnostic equipment. By using the WTC3243HB temperature controller, researchers were able to maintain consistent and stable temperatures of the capillary and the solution inside the capillary in this backscattering interferometer, beneficial for measuring molecular binding via interferometric refractive index sensing.

## REFERENCES

1. Mulkerns, N.M.C.; Hoffmann, W.H.; Lindsay, I.D.; Gersen, H. Shedding Light on Capillary-Based Backscattering Interferometry, *Sensors* **22**, 2157 (2022). <https://doi.org/10.3390/s22062157>
2. You, Z.; Jiang, D.; Stamnes, J.; Chen, J.; Xiao, J. Characteristics and applications of two-dimensional light scattering by cylindrical tubes based on ray tracing. *Appl. Opt.* **51**, 8341 (2012). <https://doi.org/10.1364/AO.51.008341>
3. Xu, Q.; Tian, W.; You, Z.; Xiao, J. Multiple beam interference model for measuring parameters of a capillary. *Appl. Opt.* **51**, 6948 (2015). <https://doi.org/10.1364/AO.54.006948>
4. Tarigan, H.J.; Neill, P.; Kenmore, C.K.; Bomhop, D.J. Capillary-scale refractive index detection by interferometric backscatter. *Anal. Chem.* **68**, 1762–1770 (1996). <https://doi.org/10.1021/ac9511455>

## USEFUL LINKS

- WTC3243HB [Product Page](#)
- WTC32ND-HB [Product Page \(New Version\)](#)

## PERMISSIONS

Figures 1, 2, 3, 4, 5, & 6 in this case study were obtained from Reference 1. The article (Ref. 1) is distributed under terms of Creative Commons Attribution 4.0 International License (<https://creativecommons.org/licenses/by/4.0/>), which permits unrestricted use, distribution, and reproduction in any medium, provided that you give appropriate credit to the original authors and the source, provide a link to the Creative Commons license, and indicate if changes were made.

A caption was added to Figure 1, and the captions in Figures 2 and 6 were edited to match format. The other images are presented here in their original form and caption.

### PRODUCTS USED

WTC3243 HB

### KEYWORDS

Backscattering interferometry, capillary, refractive index, ray tracing, polarization, fringe pattern, spatial chirps, models, WTC3243HB, temperature controller

### REVISION HISTORY

Document Number: CS-TC07

REVISION	DATE	NOTES
A	September 2022	Initial Release